Responses of the chloroplast glyoxalase system to high CO2 concentrations

Shimakawa, Ginga ; Ifuku, Kentaro ; Suzuki, Yuji ; Makino, Amane ; Ishizaki, Kimitsune ; Fukayama, Hiroshi ; Morita, Ryutaro ; Sakamoto,…

(Citation)
Bioscience, Biotechnology, and Biochemistry,82(12):2072-2083

(Issue Date)
2018-08-18

(Resource Type)
journal article

(Version)
Accepted Manuscript

(URL)
https://hdl.handle.net/20.500.14094/90006322

Running title: Glyoxalase system in chloroplasts

Online graphical abstract: The glyoxalase system scavenges methylglyoxal produced in chloroplasts during photosynthesis.

***Corresponding Author:** Ginga Shimakawa
Department of Biological and Environmental Science, Faculty of Agriculture, Graduate School of Agricultural Science, Kobe University, 1-1 Rokkodai, Nada, Kobe 657-8501, Japan
Fax: +81-78-803-5851; e-mail: ginshimakawa@gmail.com
#Present address: Institute for Integrative Biology of the Cell, Centre National de la Recherche Scientifique, Comissariat à lEnergie Atomique et aux Energies Alternatives Saclay, Institut de Biologie et de Technologie de Saclay, Université Paris-Sud, Gif-sur-Yvette, France

Author contributions: C.M. conceived the original screening and research plans; C.M. and Ke.I. supervised the experiments; G.S. and Ke.I. performed most of the experiments; Y.S., A.M., Ki.I., H.F., R.M., K.S., and A.N. provided technical assistance to G.S.; C.M., G.S., and Ke.I. designed the experiments and analysed the data; C.M. and G.S. conceived the project and wrote the manuscript.

Funding information: This work was supported by the Japan Society for the Promotion of Science (JSPS; grant no. 26450079 to C.M.), the Ministry of Education, Culture, Sports, Science, and Technology of Japan (Scientific Research in Innovative Areas, grant no. 22114512 to C.M.), and the Core Research for Evolutional Science and Technology (CREST) division of the Japan Science and Technology Agency (Grant No. AL65D21010 to C.M.). G.S. was supported as a JSPS research fellow (Grant No. 16J03443).

Title: Responses of the chloroplast glyoxalase system to high CO_2 concentrations

Authors: Ginga Shimakawa[1,#,*], Kentaro Ifuku[2,3], Yuji Suzuki[3,4,5], Amane Makino[4], Kimitsune Ishizaki[6], Hiroshi Fukayama[1], Ryutaro Morita[1], Katsuhiko Sakamoto[1], Akiko Nishi[1], and Chikahiro Miyake[1,3]

[1]Graduate School of Agricultural Science, Kobe University, 1-1 Rokkodai, Nada, Kobe 657-8501 Japan

[2]Division of Integrated Life Science, Graduate School of Biostudies, Kyoto University, Sakyo, Kyoto 606-8502 Japan

[3]Core Research for Environmental Science and Technology, Japan Science and Technology Agency, 7 Goban, Chiyoda, Tokyo 102-0076 Japan

[4]Graduate School of Agricultural Science, Tohoku University, Tsutsumidori-Amamiya, Aoba, Sendai 981-8555 Japan

[5]Faculty of Agriculture, Iwate University, Ueda 3-18-8, Morioka, Iwate 020-8550 Japan

[6]Graduate School of Science, Kobe University, 1-1 Rokkodai, Nada, Kobe 657-8501 Japan

[#]**Present address:** Institute for Integrative Biology of the Cell, Centre National de la Recherche Scientifique, Comissariat à lEnergie Atomique et aux Energies Alternativ es Saclay, Institut de Biologie et de Technologie de Saclay, Université Paris-Sud, Gif-sur-Yvette, France

Keywords: dicarbonyls; methylglyoxal; glyoxalase system; photosynthesis; high [CO_2]

Abstract

Sugar metabolism pathways such as photosynthesis produce dicarbonyls, e.g. methylglyoxal (MG), which can cause cellular damage. The glyoxalase (GLX) system comprises two enzymes GLX1 and GLX2, and detoxifies MG; however, this system is poorly understood in the chloroplast, compared with the cytosol. In the present study, we determined GLX1 and GLX2 activities in spinach chloroplasts, which constituted 40% and 10%, respectively, of the total leaf glyoxalase activity. In *Arabidopsis thaliana*, five GFP-fusion GLXs were present in the chloroplasts. Under high CO_2 concentrations, where increased photosynthesis promotes the MG production, GLX1 and GLX2 activities in *A. thaliana* increased and the expression of *AtGLX1-2* and *AtGLX2-5* was enhanced. On the basis of these findings and the phylogeny of GLX in oxygenic phototrophs, we propose that the GLX system scavenges MG produced in chloroplasts during photosynthesis.

Introduction

The substantial increase in CO_2 partial pressure in the atmosphere can cause a variety of global environmental changes. One possible effect of elevated CO_2 concentrations ($[CO_2]$) is increased photosynthetic CO_2 assimilation in plants, which may appear favourable for agricultural productivity in the near future. However, acceleration of photosynthesis by elevated $[CO_2]$ has the potential to cause dicarbonyl stress in plants.

Dicarbonyls (α-oxoaldehydes) include methylglyoxal (MG), glyoxal, and 3-deoxyglucosone, which are generated as by-products in sugar metabolism pathways in plants, including photosynthesis and respiration. Dicarbonyl MG is inevitably produced during the equilibrium reaction between glyceraldehyde 3-phosphate and dihydroxyacetone phosphate, which is catalysed by triosephosphate isomerase in both glycolysis and Calvin-Benson cycle [1,2]. Accumulated dicarbonyls react with amino acid residues (lysine and arginine) of proteins and produce advanced glycation end products (AGEs) and cause protein inactivation [3]. Thus, both photosynthesis and respiration can be associated with dicarbonyl stress.

Elevated $[CO_2]$ can enhance the risk of dicarbonyl stress due to increased photosynthetic activity. In intact plant leaves, accelerated photosynthesis by elevated $[CO_2]$ causes accumulation of sugars in the cells [4] and increase in MG production [2]. In addition, the amount of carbonylated proteins increases under high CO_2 conditions in *Arabidopsis thaliana* and soybean leaves [5]. Overall, plants are exposed to cellular damage from respiratory and photosynthetic sugar metabolism pathways, which is more profound under high $[CO_2]$.

Photosynthetic organisms have detoxifying systems that target MG similar to the corresponding mechanisms in vertebrates. These detoxifying systems are the aldo-keto

reductase (AKR) and glyoxalase (GLX) systems. AKR reduces MG to acetol with NAD(P)H as an electron donor [6]. In the C_3 plant *A. thaliana*, several AKRs that belong to the AKR4C subfamily [6], e.g., AKR4C9, has been found in chloroplasts [7]. Additionally, gene expression of the *AKR4C* subfamily members is enhanced under high light and high [CO_2] conditions [8]. In contrast, MG is non-enzymatically scavenged by reduced glutathione (GSH) to hemithioacetal (HA), and the GLX system converts HA to D-lactate. The GLX system is comprised of two enzymes, GLX1 and GLX2 [9]. GLX1 is a divalent metal-ion dependent lyase that catalyses the isomerisation of HA to *S*-D-lactoylglutathione (SLG). GLX2 is a thiolesterase that catalyses the hydrolysis of SLG to D-lactate and GSH. The major physiological substrate of GLX1 is MG, although other dicarbonyls such as glyoxal, hydroxypyruvate, and 4,5-doxovalerate are also catalysed by GLX1 [9]. The GLX system has been identified as a scavenging system for MG that is produced during glycolysis in the cytosol [9]. However, the production of MG was observed in isolated chloroplasts in a light-dependent manner [2], which suggests that the GLX system is used in chloroplasts to scavenge MG produced in photosynthesis.

We investigated the physiological significance of the GLX system in the chloroplasts of plant leaves on the basis of the above-mentioned hypothesis. We determined GLX1 and GLX2 activities in chloroplasts isolated from spinach leaves. To examine the molecular mechanisms of the chloroplast GLX system in plant leaves, we selected three GLX1 (AtGLX1-1, -2, and -3) and two GLX2 candidate genes (AtGLX2-4 and -5) based on the presence of transit peptides in the model C_3 plant *A. thaliana*. We observed the expression of GFP-AtGLX fusion proteins in chloroplasts. Additionally, we found that both activity and gene expression of the components of the GLX system in *A. thaliana* leaves were enhanced under high [CO_2], which in turn accelerated photosynthesis and dicarbonyl production.

Materials and Methods

Plant materials

Spinach was obtained from a vegetable store in Kobe, Japan. The wild-type *A. thaliana* ecotype Columbia *gl1* was grown under long-day conditions (16 h light, 23 °C, 100 μmol photons m^{-2} s^{-1}/8 h dark, 21 °C), under ambient (400 ppm), or high (2000 ppm) [CO_2] conditions. Partial CO_2 pressure was regulated using a controller device purchased from Nippon Medical and Chemical Instruments Co., LTD. (Osaka, Japan) in a closed phytotron (Biotron nc350, Nippon Medical and Chemical Instruments Co., LTD, Osaka, Japan; FLI-2000H, EYELA, Tokyo, Japan). Seeds were planted in pots filled with Metro-Mix 350 (Sun Gro Horticulture, Agawam, MA, USA), and watered with a Hyponex solution (Hyponex, Osaka, Japan). Rosette leaves were collected four weeks after germination for experimental use.

Preparation of stromal fractions from leaf chloroplasts

Intact chloroplasts were isolated from spinach and *A. thaliana* leaves using the commonly employed Percoll density gradient [10,2]. Chloroplasts were harvested by gentle centrifugation, and subsequently ruptured osmotically in extraction buffer (50 mM HEPES-KOH, 1 mM $MgCl_2$, 10 mM NaCl, 0.5 mM KH_2PO_4, 2 mM EDTA, pH 7.6). After 30 min of centrifugation at 10,000 × *g*, the supernatant containing the stromal fraction was collected. Protein concentration was measured using a Pierce 660 nm Protein Assay (Thermo Scientific, Waltham, MA, USA). Total chlorophyll (Chl) content of the chloroplast was spectroscopically measured in 80% (v/v) acetone, following the method of Arnon (1949) [11].

Preparation of total soluble proteins from plant leaves

Spinach and *A. thaliana* leaves were ground in a mortar with extraction buffer (described above) containing a protease inhibitor cocktail tablet (Complete Mini, Roche, Basel, Switzerland). After centrifugation at 10,000 × *g* for 30 min, the supernatant containing the total soluble fraction was collected. Protein concentration was measured using a Pierce 660 nm Protein Assay (Thermo Scientific, Waltham, MA, USA). Other leaf subsamples were ground in a mortar in 80% (v/v) acetone, and total Chl was spectroscopically determined following the method of Arnon (1949) [11].

Enzyme assays

GLX1 activity was measured in a 1 mL reaction mixture containing 50 mM sodium phosphate (pH 7.0), various amounts of protein (see figure and table legends), and concentrations of HA non-enzymatically formed from MG and GSH. Enzymatic activity was assessed by measuring the initial rate of SLG formation, indicated by increased absorbance at 240 nm. An ε_{240} of 2.86 mM^{-1} cm^{-1} was used to calculate GLX1 activity [12]. To measure the activity of the recombinant S6803GLX1 protein, we added 10 M of Ni^{2+} as $NiSO_4$ per mol protein to the reaction mixture.

GLX2 activity was measured in a 1 mL reaction mixture containing 50 mM Tris-HCl (pH 7.4), protein (see the figure and table legends), and various concentrations of SLG. Measurement of absorbance at 240 nm was used to assess hydrolytic activity. An ε_{240} of 3.1 mM^{-1} cm^{-1} was used to calculate GLX2 activity [12].

Preparation of recombinant AtGLX2-4 protein

The coding region was obtained from total RNA of *A. thaliana* using the KOD-plus Neo (Toyobo, Osaka, Japan) and was subcloned into the *Bam* HI site of a pGEX4T-3 vector (GE Healthcare, Little Chalfont, UK), using an In-Fusion HD Cloning Kit (Takara, Shiga, Japan). We removed the region encoding an extension of the N-terminus of AtGLX2-4, according to a comparison with the respective sequence of AtGLX2-5 [13]. The primers used are shown in the Supplemental Table S1. BL21 was used as the host cell line and the proteins were expressed at 15 °C for 16 h in Luria–Bertani broth containing 0.1 mM isopropyl-*β*-D-thiogalactopyranoside.

The harvested cells were resuspended in binding buffer (140 mM NaCl, 2.7 mM KCl, 10 mM Na_3PO_4, 1.8 mM KH_2PO_4, 1 mM phenylmethylsulfonyl fluoride, pH 7.3). The cells were mildly sonicated, and the crude extract was centrifuged at 13,000 × *g* at 4 °C for 30 min. The lysate was loaded onto GSTrap FF columns (GE Healthcare, Little Chalfont, UK) equilibrated with binding buffer. Unbound protein was removed by washing the columns with binding buffer, and GST-fusion proteins were eluted with elution buffer (50 mM Tris-HCl, 10 mM GSH, 1 mM phenylmethylsulfonyl fluoride, pH 8.0). To remove GSH, the eluted solution was loaded onto a PD-10 column (GE Healthcare, Little Chalfont, UK) in GSH-free elution buffer. The concentration of eluted proteins was measured using a Pierce 660 nm Protein Assay (Thermo Scientific, Waltham, MA, USA).

Transient expression in *A. thaliana* mesophyll protoplasts

Preparation of protoplasts from *A. thaliana* rosette leaves and PEG-calcium transfection were performed following the methods described previously [14]. The coding regions of *AtGLX1-1*,

185 *AtGLX1-2*, and *AtGLX1-3* in both transit (AtGLX1-1_1, AtGLX1-2_6, and AtGLX1-3_4;
186 Supplemental Fig. S1) and non-transit forms (AtGLX1-1_2, AtGLX1-2_2, and AtGLX1-3_2;
187 Supplemental Fig. S1) were obtained by PCR using the KOD-FX Neo (Toyobo, Osaka,
188 Japan) and were then subcloned into the *Sal*I and *Nco*I sites of a pCaMV35S_GFP vector
189 using the In-Fusion HD Cloning Kit (Takara, Shiga, Japan). For GLX2, the coding regions of
190 *GLX2-4* and *GLX2-5* were subcloned into the *Sal* I and *Nco* I sites of a pCaMV35S_GFP
191 vector, similar to the GLX1 isozymes. The primers used for cloning are shown in
192 Supplemental Table S1. For transformation, 10 μg DNA of each plasmid were transfected into
193 2×10^4 protoplasts. GFP and Chl fluorescence was observed using a fluorescence microscope
194 (BZ-8000, KEYENCE, Japan). The field of cells was excited at 480 nm and fluorescence
195 emission was measured at 510 nm.
196
197 **Real-time PCR**
198
199 Quantitative real time-PCR was performed using SYBR Premix Ex Taq (Takara, Shiga,
200 Japan) and a LightCycler 1.5 (Roche, Basel, Switzerland). A comparative threshold cycle
201 method was applied to determine relative concentrations of mRNA. The primers used are
202 shown in Supplemental Table S1. We used the Arabidopsis actin gene, *actin2*, as a reference
203 gene, and the obtained data were normalised to *actin2* using the ΔΔCT method [15].
204
205 **Phylogenetic analysis**
206
207 Sequences were aligned using ClustalW. The sequence comparisons were performed only in
208 the Glyoxalase domain in the N-terminus of GLX1 and the hydroxyacylglutathione hydrolase
209 domain in the C-terminus of GLX2, both of which were predicted from the Pfam database.

The amino acid sequences of GLX1 and GLX2 were obtained from CyanoBase (Slr0381 for S6803GLX1; Sll1019 for S6803GLX2), the National Center for Biotechnology Information (XP_005849034 for CvGLX1-1; XP_005847305 for CvGLX1-2; XP_005535468 for CmGLX1; XP_002180432 for PtGLX1; WP_029404302 for EcGLX1; ONH72282 for ScGLX1; XP_005845456 for CvGLX2; XP_005539165 for CmGLX2; XP_002185216 for PtGLX2; WP_063077511 for EcGLX2; KZV12511 for ScGLX2), the MarpolBase (Mapoly0020s0109 for MpGLX1-1; Mapoly0033s0085 for MpGLX1-2; Mapoly0033s0083 for MpGLX1-3; Mapoly0204s0005 for MpGLX2-1; Mapoly0204s0009 for MpGLX2-2), Phytozome (402441 for SmGLX1-1; 270490 for SmGLX1-2; 164521 for SmGLX2-1; 149526 for SmGLX2-2; Os02g17920 for OsGLX1-1; Os08g09250 for OsGLX1-2; Os05g14194 for OsGLX1-3; Os05g22970 for OsGLX1-4; Os09g34100 for OsGLX2-1; Os03g21460 for OsGLX2-2; Zm00008a021415 for ZmGLX1-1; Zm00008a015465 for ZmGLX1-2; Zm00008a039630 for ZmGLX1-3; Zm00008a025479 for ZmGLX1-4; Zm00008a007714 for ZmGLX1-5; Zm00008a028591 for ZmGLX2-1; Zm00008a001400 for ZmGLX2-2), and TAIR (Table 2).

Phylogenetic trees for GLX1 and GLX2 were constructed using MEGA7, based on the sequence alignments in Supplemental Fig. S3 and S4 [16]. The evolutionary history was inferred using a neighbour-joining method. The percentages of replicate trees in which the associated taxa clustered together in the bootstrap test are indicated near the respective branches. The tree was drawn to scale, with branch lengths in the same units as those of the evolutionary distances used to infer the phylogenetic tree. Evolutionary distances were computed using the Poisson correction method based on the number of amino acid substitutions per site.

Results

GLX1 and GLX2 activity in spinach chloroplasts

We measured GLX1 and GLX2 activities in the stromal fraction of spinach chloroplasts and compared these activities with the respective enzymatic activity in the total soluble fraction of spinach leaves. In the total soluble fraction extracted from spinach leaves, we found similar maximum activity of GLX1 and GLX2 per total soluble protein content (Fig. 1A and B). However, in the spinach chloroplast stromal fraction, the activity of GLX1 per total stromal protein was larger than that of GLX2 (Fig. 1A and B). No enzymatic activity of both GLX1 and GLX2 was measurable after 10 min of boiling. These results indicate that GLX1 and GLXs are active in the stroma extracts, and that GLX1 activity is higher than GLX2 activity.

Subsequently, we calculated GLX1 and GLX2 activity in the total soluble and stromal fractions as values per total Chl content, based on the ratios of leaf soluble protein to Chl (3.5 ± 0.4 mg leaf soluble protein mg^{-1} Chl, $n = 3$) and stromal protein to Chl (1.89 ± 0.08 mg stromal protein mg^{-1} Chl, $n = 3$), in spinach leaves. For this, we evaluated GLX activity in both fractions based on the same parameter, i.e., total Chl content (Fig. 1C and D) as all Chl in spinach leaves should originate from chloroplasts. The maximum activities (V_{max}) of GLX1 and GLX2 in the leaf soluble fraction were 45 ± 5 and 60 ± 8 μmol SLG (mg Chl)$^{-1}$ h^{-1} (n = 3), respectively (Table 1). Additionally, the K_m for the HA or SLG substrates were 0.046 ± 0.014 and 0.21 ± 0.06 mM (n = 3) in the leaf soluble fraction, respectively (Table 1). In contrast, in the chloroplast extracts, V_{max} and K_m of the GLX1 reaction were 16 ± 2 μmol SLG (mg Chl)$^{-1}$ h^{-1} and 0.072 ± 0.017 mM (n = 3), and those of the GLX2 reaction were 4.8 ± 0.4 μmol SLG (mg Chl)$^{-1}$ h^{-1} and 0.12 ± 0.03 mM (n = 3), respectively (Table 1). These results indicate that approximately 40% of GLX1 and 10% of GLX2 activity in spinach leaves

258 originated from the chloroplasts.

259

260 **Characteristics of GLX1 and GLX2 in *A. thaliana***

261

262 To investigate the molecular mechanism of the chloroplast GLX system in leaves, we used the
263 model C_3 plant *A. thaliana*, which has three isozymes of GLX1 (Table 2). Based on the
264 primary structure, these three GLX1 isozymes are categorised into two metal-dependent
265 classes, Ni^{2+}-dependent (AtGLX1-1 and -2) and Zn^{2+}-dependent enzymes (AtGLX1-3) [17].
266 Furthermore, all three GLX1 isozymes have splice variants with transit peptides
267 (AtGLX1-1_1, AtGLX1-2_6, and AtGLX1-3_4; Supplemental Fig. S1) that are predicted to
268 be localised in chloroplasts [17]. Moreover, these AtGLX1s show isomerisation activity for
269 HA to SLG (Table 2) [18].

270 There are five GLX2 isozymes (AtGLX2-1, -2, -3, -4, and -5) that are annotated
271 based on the primary structure in *A. thaliana* (Table 2). All isozymes, except GLX2-2, have
272 putative transit peptides [18]. It has previously been reported that recombinant AtGLX2-2 and
273 -5 proteins show GLX2 activity (Table 2) [13,19,20], and that AtGLX2-1 and -3 possess no
274 SLG hydrolysis activity and do not function in the GLX system [20,21]. To the best of our
275 knowledge, the present study is the first to determine GLX2 activity of the glutathione
276 *S*-transferase (GST)-tagged AtGLX2-4 recombinant protein. K_m was 0.24 ± 0.02 mM and k_{cat}
277 was 19000 ± 5000 min^{-1} (n = 3; Table 2). Taken together, our results show that AtGLX2-4
278 possesses GLX2 activity as well as AtGLX2-2 and -5.

279

280 **Subcellular localisation of GLX1 and GLX2 in *A. thaliana***

281

282 We examined subcellular localisation of five GLX isozymes with transit peptides, including

AtGLX1-1, -2, and -3 (i.e., AtGLX1-1_1, AtGLX1-2_6, and AtGLX1-3_4; Supplemental Fig. S1), and AtGLX2-4 and -5 in *A. thaliana*. These five GLXs were transiently expressed in *A. thaliana* mesophyll protoplasts as GFP-fusion proteins. The GFP fluorescence from all five GLX constructs was exclusively detected in chloroplasts, which were identified by the red auto-fluorescence of Chl (Fig. 2). These results suggest that the three GLX1 isozymes (AtGLX1-1, -2, and -3) and the two GLX2 isozymes (AtGLX2-4 and -5) are located in the chloroplasts of *A. thaliana* mesophyll cells.

All three GLX1 isozymes in *A. thaliana* have splice variants that have no N-terminal transit peptide (Supplemental Fig. S1). Thus, AtGLX1-1, -2, and -3 were assumed to be expressed not only with transit peptides but also without transit peptides. Furthermore, we investigated the subcellular localisation by transiently expressing GFP-fusion constructs of AtGLX1-1, -2, and -3, which lacked the transit peptide (AtGLX1-1_2, AtGLX1-2_2, and AtGLX1-3_2), designated as AtGLX1-1w/oS, AtGLX1-2w/oS, and AtGLX1-3w/oS, respectively. We detected GFP fluorescence around chloroplasts (Supplemental Fig. S2). These results suggest that splice variants of these GLX1 isozymes exist in the cytosol of *A. thaliana* mesophyll cells.

Responses of GLX1 and GLX2 to high [CO_2] in *A. thaliana*

To investigate the responses of the chloroplast GLX system to high [CO_2], we measured GLX1 and GLX2 activity in *A. thaliana* leaves grown under atmospheric and high [CO_2] conditions. Both GLX1 and GLX2 activities in the soluble fraction of the *A. thaliana* leaves were significantly higher in plants grown under high [CO_2] than in plants grown under atmospheric [CO_2] (Fig. 3A).

Furthermore, we investigated the expression of the genes encoding AtGLXs. The

308 expression of *AtGLX1-2* and *AtGLX2-5* was significantly increased under high [CO_2] growth
309 conditions (Fig. 3B). The gene for *AtGLX1-2* showed the highest expression levels under high
310 [CO_2], which was approximately four-fold that measured under atmospheric conditions (Fig.
311 3B).
312
313 **Phylogeny of GLX1 and GLX2 in oxygenic phototrophs**
314
315 The production of MG derived from photosynthesis [2] implies that oxygenic phototrophs
316 require the GLX system in chloroplasts. In fact, GLX1 and GLX2 activities were observed in
317 the stromal fraction of spinach chloroplasts (Fig. 1 and Table 1). Furthermore, three GLX1
318 isozymes, AtGLX1-1, -2, and -3, and two GLX2 isozymes, AtGLX2-4 and -5, were detected
319 in the chloroplasts of *A. thaliana* (Fig. 2). Reportedly, AtGLX2-2, which does not possess a
320 transit peptide, is exclusively located in the cytosol [18, 20, 21]. Previously, we characterised
321 the GLX system in the cyanobacterium *Synechocystis* sp. PCC 6803 (S. 6803) [22],
322 suggesting that the chloroplast GLX system may have originated from cyanobacteria, which
323 are the ancestors of chloroplasts of plants. In the present study, we compared the primary
324 structures of GLX1 and GLX2 between the heterotrophic prokaryote *Escherichia coli*,
325 eukaryote *Saccharomyces cerevisiae*, and a variety of oxygenic phototrophs, including S.
326 6803, the green alga *Chlorella variabilis*, the liverwort *Marchantia polymorpha*, the fern
327 *Selaginella moellendorffii*, *A. thaliana*, the C_3 plant *Oryza sativa*, the C_4 plant *Zea mays*, the
328 red alga *Cyanidioschyzon merolae*, and the diatom *Phaeodactylum tricornutum* (Supplemental
329 Figs. S3 and S4) to evaluate the phylogeny of the GLX system in oxygenic phototrophs. The
330 phylogenetic tree of GLX1 clearly showed the division of two groups with Ni^{2+}- and
331 Zn^{2+}-dependent GLX1s (Fig. 4). The activity of cyanobacterial GLX1 was biochemically
332 characterised to be a Ni^{2+}-dependent type [16,22] (Supplemental Table S2). Both GLX1s in S.

6803 and *E. coli* were separate from the other Ni^{2+}-dependent GLX1 in the phylogenetic tree (Fig. 4); this suggests that the primary structure of GLX1 has largely varied in the evolution of these eukaryotes. Compared with Ni^{2+}-dependent GLX1, the phylogeny of Zn^{2+}-dependent GLX1 is likely to follow the evolutionary lineage of oxygenic phototrophs from cyanobacteria to angiosperms (Fig. 4). The green alga *C. variabilis* and land plants have both Ni^{2+}- and Zn^{2+}-dependent GLX1 isozymes, whereas the red alga *C. merolae* and the diatom *P. tricornutum* have only the Zn^{2+}-dependent isoform, similarly to heterotrophs, *E. coli* and *S. cerevisiae* (Fig. 4). In contrast, the phylogenetic tree of GLX2 showed a distinct division of AtGLX2 into two groups. Both AtGLX2-4 and -5 detected in chloroplasts (Fig. 2); and AtGLX2-2 located in the cytoplasm [18]. Interestingly, the C_3 plant *O. sativa* and the C_4 plant *Z. mays* possess GLX2 isozymes similar to AtGLX2-4 or -5 (OsGLX2-1 and ZmGLX2-1, respectively; Fig. 5), which are presumably located in chloroplasts. Moreover, both *O. sativa* and *Z. mays* show GLX2 (OsGLX2-2 and ZmGLX2-2) to be homologous to AtGLX2-2 (Fig. 5). These results suggest a categorisation into chloroplastic and cytoplasmatic GLX2 isozymes, which may occur in all angiosperms. The liverwort *M. polymorpha* and the fern *S. moellendorffii* have two isozymes of GLX2, whereas the genomes of the eukaryotic algae *C. variabilis*, *C. merolae*, and *P. tricornutum* contain only one gene encoding GLX2 (Fig. 5), suggesting that GLX2 is used only in the cytosol in these algae unless GLX2 is expressed in various forms and exists both in cytosol and chloroplasts, similar to AtGLX1-1, -2, and -3 (Fig. 2 and Supplemental Fig. 2).

353 **Discussion**

354

355 In the present study, we characterised the chloroplast-localised GLX system and investigated
356 its response to high [CO_2] conditions. GLX1 and GLX2 activities in the stromal fraction were
357 estimated at approximately 40% and 10%, respectively, of that measured in the total soluble
358 fraction in spinach leaves (Fig. 1 and Table 1). This indicates that the chloroplast GLX system
359 participates in the dynamic cellular metabolism of MG that is probably produced during
360 photosynthesis. In *A. thaliana*, three AtGLX1s (AtGLX1-1, -2, and -3) fused with GFP were
361 found in the chloroplasts of mesophyll protoplasts of *A. thaliana* (Fig. 2). The GFP-fusion
362 constructs of AtGLX2-4 and -5 observed in chloroplasts (Fig. 2) were different from the
363 cytosolic AtGLX2-2 isozyme. From these data, we summarised the metabolic pathway of MG
364 in the GLX system in *A. thaliana* (Fig. 6). The GLX system has been known to be present in
365 the cytosol where it scavenges MG produced during glycolysis [9]. However, photosynthetic
366 CO_2 assimilation stimulates MG production [2]. Furthermore, proteome analysis using mass
367 spectrometry showed AtGLX1-1 and -3 in the chloroplasts of *A. thaliana* [23]. These results
368 support the hypothesis of the present study. Recently, Schmitz et al. (2017) measured
369 YFP-GLX isozyme fusion constructs expressed in tobacco leaves by *Agrobacterium* leaf
370 infiltration to show that three AtGLXs (i.e., AtGLX1-1 and -3, and AtGLX2-5) are present in
371 chloroplasts. In general, our results are consistent with this study. However, Schmitz et al.
372 (2017) concluded that AtGLX1-2 and AtGLX2-4 are present in the endoplasmic reticulum
373 and mitochondria, respectively. This discrepancy might be attributed to the different
374 transformation methods used. Furthermore, we used the protoplast of *A. thaliana* as the host
375 cell to express AtGLXs fused with GFP, which differs from that of tobacco in the
376 above-mentioned study [18]. In spinach chloroplasts, GLX1 activity was higher than that of
377 GLX2 (Fig. 1 and Table 1), suggesting that a part of SLG (with GSH) may be exported from

chloroplasts into the cytosol. In addition, GLX2 activity has been detected in the mitochondrial matrix of spinach leaves, and furthermore, the final product of the GLX system, D-lactate, is metabolised to pyruvate by D-lactate dehydrogenase in the mitochondria [24]. The coordinate metabolism of chloroplasts, the cytosol, and mitochondria for scavenging MG likely include dynamic redox signalling across these organelles. Taken together, the GLX system in plant leaves occurs in chloroplasts and is up-regulated to alleviate dicarbonyl stress under high [CO_2].

Alternative splicing may regulate the compartmentalisation of GLX1 activity between chloroplasts and the cytosol. It has been reported that approximately 60% of the *A. thaliana* genes are alternatively spliced and one third of those are functional [25]. Three GLX1 isozymes in *A. thaliana* have splice variants located in the cytosol (Supplemental Fig. S2), as well as variants that include transit peptides for their expression in chloroplasts (Fig. 2). These data are consistent with the findings of Schmitz et al. (2017). At night, photosynthetic CO_2 assimilation ceases and the concentration of triose phosphates such as glyceraldehyde 3-phosphate and dihydroxyacetone phosphate in chloroplasts is lower than that under light conditions [26]. Therefore, the chloroplast GLX system is presumably required during daytime, but not during night time. Further research is needed to elucidate the dependence of the modulation of GLX1 activity on photosynthetic activity between the organelles.

An increase in [CO_2] can accelerate dicarbonyl stress despite enhanced GLX system activity. Atmospheric [CO_2] has been increasing and thus affecting plants. Under high [CO_2] soluble sugars such as D-glucose accumulate in plant cells [4], which promotes the production of MG [2]. We found that both GLX1 and GLX2 activities were enhanced (Fig. 3A) and the genes encoding AtGLX1-2 and AtGLX2-5 were highly expressed (Fig. 3B) under high [CO_2] conditions. These data are consistent with the increase of expression of genes associated with

403 the GLX system in response to high levels of sugar [18] and MG [27]. Overall, the GLX
404 system is supposed to prevent the accumulation of MG in cells under high [CO_2] conditions.
405 Nevertheless, this carbonylated protein can accumulate under high [CO_2] even in wild-type
406 plants [5], suggesting that plant leaves are exposed to dicarbonyl stress under high [CO_2],
407 even if the GLX system is upregulated. Further enhancement of the GLX system through
408 genetic modification and additive agents might facilitate avoidance of disadvantageous
409 accumulation of MG under high [CO_2] conditions [27]. In the present study, no significant
410 differences were found in the expression levels of *AtGLX1-1, AtGLX1-3*, or *AtGLX2-4* genes
411 between atmospheric and high [CO_2] (Fig. 3B), which may suggest that these GLX isozymes
412 respond to variations in other natural environmental factors, such as high light intensity [18].
413 There are diverse scavenging systems for MG in chloroplasts. One of the most
414 prominent mechanisms is AKR. Previously, Saito et al. (2011) verified the
415 NADPH-dependent reducing activity of MG in the stromal fraction of spinach chloroplasts.
416 The K_m and V_{max} values for MG were 6.5 mM and 3.3 μmol MG (mg Chl)$^{-1}$ h^{-1}, respectively.
417 In *A. thaliana*, AKR4C9, a member of the AKR4C subfamily, had a k_{cat}/K_m value of
418 approximately 10^2–10^3 mM^{-1} min^{-1} for scavenging MG [6,8] and was located in the
419 chloroplasts [7]. The expression of the *AKR4C* subfamily was enhanced in response to high
420 light and high CO_2 [8]. This indicates that AKR may detoxify MG produced during
421 photosynthesis. In contrast, the short- and medium-chain dehydrogenases/reductases SDR and
422 MDR, respectively, can reduce MG to acetol with NADPH as the electron donor, similarly to
423 AKR [7,22]. Both SDR and MDR are broadly conserved in oxygenic phototrophs; however,
424 the NADPH-dependent MG reducing activities of the recombinant proteins are significantly
425 lower in plant leaves than in cyanobacteria [22]. In the present study, GLX1 and GLX2
426 activities in the chloroplasts of spinach leaves (Fig. 1 and Table 1) had lower K_m and higher
427 V_{max} than the NADPH-dependent MG reducing reaction. In chloroplasts, MG can rapidly

accumulate to a high level when the detoxification efficiency is low because the production rate of MG during photosynthesis is approximately 3% of the photosynthetic O_2 evolution rate [2]. High cellular accumulation of MG (e.g. mM-order) inhibits plant growth [28]. However, the lack of a GLX isozyme does not inhibit plant growth [18], most likely because oxygenic phototrophs have developed a variety of complementary systems for controlling MG accumulation.

The chloroplast GLX system might have developed during the evolutionary history of oxygenic phototrophs. In the present study, we phylogenetically analysed GLX1 and GLX2 of different oxygenic phototrophs, including S. 6803, *C. variabilis*, *M. polymorpha*, *S. moellendorffii*, *A. thaliana*, *O. sativa*, *Z. mays*, *C. merolae*, and *P. tricornutum*. Cyanobacteria are the progenitors of oxygenic photosynthesis and contain the GLX system (Fig. 4 and 5) [22], which implies that photosynthetic organisms developed the GLX system for scavenging MG originating from the Calvin-Benson cycle as oxygenic phototrophs and conserved and diversified the GLX system over their evolutionary history (Fig. 4 and 5). Generally, green algae, red algae, and land plants, termed Archaeplastida, are assigned to one group, which has experienced a single endosymbiotic event. Nevertheless, the red alga *C. merolae* and *P. tricornutum* only have a Zn^{2+}-dependent GLX1 (Fig. 4). These oxygenic phototrophs can be also termed as red plastid lineage and known to have evolved differently from green algae and land plants (so-called green plastid lineage) [29]. Possibly, Ni^{2+}-dependent GLX1 had been inherited from cyanobacteria selectively to the oxygenic phototrophs in green plastid lineage. The eukaryotic algae *C. variabilis*, *C. merolae*, and *P. tricornutum* have only one GLX2, whereas land plants produce more than two isozymes of GLX2 (Fig. 5), indicating that the chloroplastic GLX system may have been established in the evolutionary process from algae to land plants. Adaption to terrestrial life may have required oxygenic phototrophs to enhance their cellular MG scavenging system, because excretion of dicarbonyls is presumably more

453 difficult in the terrestrial environment than in the aquatic environment. However, notably, CO_2
454 availability differs between the atmosphere, fresh water, and sea water. Thus, C_4 plants and
455 many algae developed CO_2-concentrating mechanisms to increase fixation efficiency [30].
456 This again might affect the scavenging systems for dicarbonyls such as the GLX system.
457 Enzyme activity, subcellular localisation, and physiological significance of the GLX system in
458 diverse oxygenic phototrophs should be assessed simultaneously with their photosynthetic
459 physiology in future studies.

460 As a trade-off for the benefits derived from photosynthesis, oxygenic phototrophs are
461 exposed to a variety of risks from oxidative stress. The dicarbonyl MG is produced in the
462 Calvin-Benson cycle [2], which accepts electrons from the photosynthetic electron transport
463 system of photosystem I (PSI) on the thylakoid membrane to form MG radicals, finally
464 reducing O_2 to a superoxide anion radical (O_2^-) [31]. Thus, MG accumulates in the
465 chloroplasts and elicits the production of reactive oxygen species (ROS), which can cause
466 oxidative damage in photosynthetic cells. In chloroplasts, ROS can also be generated due to
467 the excitation energy in photosystems I and II, which can then impair the growth of oxygenic
468 phototrophs [32,33]. Further, ROS can react with membrane lipids and free fatty acids to
469 produce α,β-unsaturated carbonyls such as acrolein [34], which can also inhibit growth of
470 oxygenic phototrophs [35]. In general, oxygenic phototrophs developed defence mechanisms
471 against the effects of ROS and dicarbonyl stress. The large amount of GSH (3.5 mM) in
472 chloroplasts [36] may play an essential role for the detoxification mechanisms of not only
473 ROS but also MG in chloroplasts. Nevertheless, predicted increases in [CO_2] and global
474 warming potentially threaten plant growth, and may cause dicarbonyl stress, known as “plant
475 diabetes” [37, 38]. The physiological significance of scavenging systems of dicarbonyls in
476 chloroplasts thus provides insight into the acclimation of plants to high [CO_2] conditions and
477 will aid in developing future agricultural and biotechnological strategies.

Acknowledgements

We would like to thank Editage (www.editage.jp) for English language editing.

Conflict of interest

The authors have no conflict of interest to declare.

Supporting information

Supplemental Table S1. Primers used in this study

Supplemental Table S2. Kinetic parameters of the recombinant S6803GLX1

Supplemental Fig. S1. Amino acid sequences of each splice variant of AtGLX1s

Supplemental Fig. S2. Subcellular localisation of AtGLX1w/oS-GFP fusion proteins in *A. thaliana* mesophyll protoplasts

Supplemental Fig. S3. Sequence comparison of the glyoxalase domain in the N-terminus of glyoxalase I

Supplemental Fig. S4. Sequence comparison of the hydroxyacylglutathione hydrolase domain in the C-terminus of glyoxalase II

496 **References**

497

498 1. Phillips SA, Thornalley PJ. The formation of methylglyoxal from triose phosphates. Eur J
499 Biochem. 1993;212:101-105.

500 2. Takagi D, Inoue H, Odawara M, Shimakawa G, Miyake C. The Calvin cycle inevitably
501 produces sugar-derived reactive carbonyl methylglyoxal during photosynthesis: a
502 potential cause of plant diabetes. Plant Cell Physiol. 2014;55:333-340.

503 3. Ahmed N, Thornalley PJ. Advanced glycation endproducts: what is their relevance to
504 diabetic complications? Diabetes Obes Metab. 2007;9:233-245.

505 4. Markelz RJC, Vosseller LN, Leakey ADB. Developmental stage specificity of
506 transcriptional, biochemical and CO_2 efflux responses of leaf dark respiration to growth
507 of *Arabidopsis thaliana* at elevated [CO_2]. Plant Cell Environ. 2014;37:2542-2552.

508 5. Qiu Q-S, Huber JL, Booker FL, Jain V, Leakey ADB, Fiscus EL, Yau PM, Ort DR,
509 Huber SC. Increased protein carbonylation in leaves of Arabidopsis and soybean in
510 response to elevated [CO_2]. Photosynth Res. 2008;97:155.

511 6. Simpson PJ, Tantitadapitak C, Reed AM, Mather OC, Bunce CM, White SA, Ride JP.
512 Characterization of two novel aldo–keto reductases from Arabidopsis: Expression
513 patterns, broad substrate specificity, and an open active-site structure suggest a role in
514 toxicant metabolism following stress. J Mol Biol. 2009;392:465-480.

515 7. Yamauchi Y, Hasegawa A, Taninaka A, Mizutani M, Sugimoto Y. NADPH-dependent
516 reductases involved in the detoxification of reactive carbonyls in plants. J Biol Chem.
517 2011;286:6999-7009.

518 8. Saito R, Shimakawa G, Nishi A, Iwamoto T, Sakamoto K, Yamamoto H, Amako K,
519 Makino A, Miyake C. Functional analysis of the AKR4C subfamily of *Arabidopsis*
520 *thaliana*: model structures, substrate specificity, acrolein toxicity, and responses to light

521 and [CO_2]. Biosci Biotechnol Biochem. 2013;77:2038-2045.
522 9. Thornalley PJ. The glyoxalase system in health and disease. Mol Aspects Med.
523 1993;14:287-371.
524 10. Lilley RM, Fitzgerald MP, Rienits KG, Walker DA. Criteria of intactness and the
525 photosynthetic activity of spinach chloroplast preparations. New Phytol. 1975;75:1-10.
526 11. Arnon DI. Copper enzymes in isolated chloroplasts. Polyphenoloxidase in *Beta vulgaris*.
527 Plant Physiol. 1949;24:1-15.
528 12. McLellan AC, Thornalley PJ. Glyoxalase activity in human red blood cells fractioned by
529 age. Mech Ageing Dev. 1989;48:63-71.
530 13. Marasinghe GPK, Sander IM, Bennett B, Periyannan G, Yang K-W, Makaroff CA,
531 Crowder MW. Structural studies on a mitochondrial glyoxalase II. J Biol Chem.
532 2005;280:40668-40675.
533 14. Yoo S-D, Cho Y-H, Sheen J. Arabidopsis mesophyll protoplasts: a versatile cell system
534 for transient gene expression analysis. Nat Protoc. 2007;2:1565.
535 15. Livak KJ, Schmittgen TD. Analysis of relative gene expression data using real-time
536 quantitative PCR and the 2-ΔΔCT method. Methods. 2001;25:402-408.
537 16. Kumar S, Stecher G, Tamura K. MEGA7: Molecular evolutionary genetics analysis
538 version 7.0 for bigger datasets. Mol Biol Evol. 2016;33:1870-1874.
539 17. Kaur C, Vishnoi A, Ariyadasa TU, Bhattacharya A, Singla-Pareek SL, Sopory SK.
540 Episodes of horizontal gene-transfer and gene-fusion led to co-existence of different
541 metal-ion specific glyoxalase I. Sci Rep. 2013;3:3076.
542 18. Schmitz J, Dittmar IC, Brockmann JD, Schmidt M, Hüdig M, Rossoni AW, Maurino VG.
543 Defense against reactive carbonyl species involves at least three subcellular
544 compartments where individual components of the system respond to cellular sugar status.
545 Plant Cell. 2017;inpress. doi:10.1105/tpc.17.00258.

19. Ridderstrom M, Mannervik B. Molecular cloning and characterization of the thiolesterase glyoxalase II from *Arabidopsis thaliana*. Biochem J. 1997;322:449-454.
20. Limphong P, Adams NE, Rouhier MF, McKinney RM, Naylor M, Bennett B, Makaroff CA, Crowder MW. Converting GLX2-1 into an active glyoxalase II. Biochemistry. 2010;49:8228-8236.
21. Devanathan S, Erban A, Perez-Torres R, Jr., Kopka J, Makaroff CA. *Arabidopsis thaliana* Glyoxalase 2-1 is required during abiotic stress but is not essential under normal plant growth. PLoS One. 2014;9:e95971.
22. Shimakawa G, Suzuki M, Yamamoto E, Nishi A, Saito R, Sakamoto K, Yamamoto H, Makino A, Miyake C. Scavenging systems for reactive carbonyls in the cyanobacterium *Synechocystis* sp. PCC 6803. Biosci Biotechnol Biochem. 2013;77:2441-2448.
23. Ferro M, Brugière S, Salvi D, Seigneurin-Berny D, Court M, Moyet L, Ramus C, Miras S, Mellal M, Le Gall S, et al. AT_CHLORO, a comprehensive chloroplast proteome database with subplastidial localization and curated information on envelope proteins. Mol Cell Proteomics. 2010;9:1063-1084.
24. Engqvist M, Drincovich MF, Flügge U-I, Maurino VG. Two D-2-hydroxy-acid dehydrogenases in *Arabidopsis thaliana* with catalytic capacities to participate in the last reactions of the methylglyoxal and β-oxidation pathways. J Biol Chem. 2009;284:25026-25037.
25. Stamm S, Ben-Ari S, Rafalska I, Tang Y, Zhang Z, Toiber D, Thanaraj TA, Soreq H. Function of alternative splicing. Gene. 2005;344:1-20.
26. Sassenrath-Cole GF, Pearcy RW. The role of ribulose-1,5-bisphosphate regeneration in the induction requirement of photosynthetic CO_2 exchange under transient light conditions. Plant Physiol. 1992;99:227-234.
27. Mustafiz A, Ghosh A, Tripathi AK, Kaur C, Ganguly AK, Bhavesh NS, Tripathi JK,

571 Pareek A, Sopory SK, Singla-Pareek SL. A unique Ni^{2+}-dependent and
572 methylglyoxal-inducible rice glyoxalase I possesses a single active site and functions in
573 abiotic stress response. Plant J. 2014;78:951-963.
574 28. Yadav SK, Singla-Pareek SL, Ray M, Reddy MK, Sopory SK. Methylglyoxal levels in
575 plants under salinity stress are dependent on glyoxalase I and glutathione. Biochem
576 Biophys Res Commun. 2005;337:61-67.
577 29. Falkowski PG, Katz ME, Knoll AH, Quigg A, Raven JA, Schofield O, Taylor FJR. The
578 evolution of modern eukaryotic phytoplankton. Science. 2004;305:354-360.
579 30. Raven JA, Beardall J, Giordano M. Energy costs of carbon dioxide concentrating
580 mechanisms in aquatic organisms. Photosynth Res. 2014;121:111-124.
581 31. Saito R, Yamamoto H, Makino A, Sugimoto T, Miyake C. Methylglyoxal functions as
582 Hill oxidant and stimulates the photoreduction of O_2 at photosystem I: a symptom of
583 plant diabetes. Plant Cell Environ. 2011;34:1454-1464.
584 32. Krieger-Liszkay A. Singlet oxygen production in photosynthesis. J Exp Bot.
585 2005;56:337-346.
586 33. Shimakawa G, Shaku K, Miyake C. Oxidation of P700 in photosystem I is essential for
587 the growth of cyanobacteria. Plant Physiol. 2016;172:1443-1450.
588 34. Mano J, Khorobrykh S, Matsui K, Iijima Y, Sakurai N, Suzuki H, Shibata D. Acrolein is
589 formed from trienoic fatty acids in chloroplast: A targeted metabolomics approach. Plant
590 Biotechnol. 2014;31:535-543.
591 35. Shimakawa G, Iwamoto T, Mabuchi T, Saito R, Yamamoto H, Amako K, Sugimoto T,
592 Makino A, Miyake C. Acrolein, an α,β-unsaturated carbonyl, inhibits both growth and
593 PSII activity in the cyanobacterium *Synechocystis* sp. PCC 6803. Biosci Biotechnol
594 Biochem. 2013;77:1655-1660.
595 36. Foyer CH, Halliwell B. The presence of glutathione and glutathione reductase in

596 chloroplasts: A proposed role in ascorbic acid metabolism. Planta. 1976;133:21-25.
597 37. Shimakawa G, Kohara A, Miyake C. Medium-chain dehydrogenase/reductase and
598 aldo-keto reductase scavenge reactive carbonyls in *Synechocystis* sp. PCC 6803. FEBS
599 Lett. 2018;592:1010-1019.
600 38. Shimakawa G, Suzuki M, Yamamoto E, Saito R, Iwamoto T, Nishi A, Miyake C. Why
601 don't plants have diabetes? Systems for scavenging reactive carbonyls in photosynthetic
602 organisms. Biochem Soc Trans. 2014;42:543-547.

603 **Tables**

Table 1. Comparison of glyoxalase (GLX) 1 and 2 activity between spinach leaves and chloroplasts

	K_m (mM)	V_{max} (μmol SLG [mg chlorophyll]$^{-1}$ h^{-1})
GLX1		
Leaves	0.046 ± 0.014	45 ± 5
Chloroplasts	0.072 ± 0.017	16 ± 2
GLX2		
Leaves	0.21 ± 0.06	60 ± 8
Chloroplasts	0.12 ± 0.03	4.8 ± 0.4

For the measurements, hemithioacetal (HA) and *S*-D-lactoylglutathione (SLG) were used as the substrates for GLX1 and GLX2, respectively. Data are means ± SD from three independent experiments.

604

Table 2. Characteristics of glyoxalase (GLX) 1 and 2 in *A. thaliana*

Name	Locus	Transit peptide	Kinetic parameters of the recombinant protein		
			K_m (mM)	k_{cat} (min^{-1})	k_{cat}/K_m (mM^{-1} min^{-1})
GLX1					
AtGLX1-1	At1g67280	+	[a]0.279 ± 0.004	[a]530 ± 30	[a]1900
AtGLX1-2	At1g11840	+	[a]0.330 ± 0.010	[a]550 ± 40	[a]2100
AtGLX1-3	At1g08110	+	[a]0.476 ± 0.125	[a]10500 ± 1800	[a]22100
GLX2					
AtGLX2-1	At2g43430	+		No GLX2 activity	
AtGLX2-2	At3g10850	−	[c]0.098 ± 0.007	[c]28000 ± 500	[c]282000
AtGLX2-3	At1g53580	+		No GLX2 activity	
AtGLX2-4	At1g06130	+	0.24 ± 0.02	19000 ± 5000	80000
AtGLX2-5	At2g31350	+	[e]0.27 ± 0.06	[e]10800 ± 1200	[e]40000

For the measurement of the recombinant AtGLX2-4 protein (0.2 μg mL^{-1}), *S*-D-lactoylglutathione was used as the substrate. Data are means ± SD from three independent experiments. Notes: [a]Schmitz et al. (2017) [18]; [b]Ridderström and Mannervik (1997) [19]; and [c]Limphong et al. (2010) [20].

605

606 **Figure legends**

607

608 **Fig. 1.** Dependence of the substrates in the soluble extracts (20 μg protein mL^{-1}) from spinach
609 leaves (grey circles) and chloroplasts (green triangles) on glyoxalase (GLX) 1 (A, C) and 2 (B,
610 D) activities. The activity was estimated based on the amounts of protein (A, B) or
611 chlorophyll (Chl) (C, D). The substrates hemithioacetal (HA) and *S*-D-lactoylglutathione
612 (SLG) were used; the production and consumption rates of SLG were measured for GLX1
613 and GLX2 activity, respectively. Data are presented as means ± SD from three independent
614 experiments.

615

616 **Fig. 2.** Subcellular localisation of the GFP-fused glyoxalase (GLX) 1 and 2 proteins
617 expressed in transiently transformed *A. thaliana* mesophyll protoplasts. Fluorescent images of
618 GFP (F_{GFP}), chlorophyll autofluorescence (F_{Chl}), and bright field (BF) are shown. Free GFP
619 protein was used as a control. Black bars = 10 μm.

620

621 **Fig. 3.** Activity (A) and expression (B) of glyoxalase (GLX) 1 and 2 in *A. thaliana* leaves in
622 response to the increase in ambient [CO_2]. Wild-type plants were grown at atmospheric (400
623 ppm, grey bars) and high (2000 ppm, dark grey bars) [CO_2]. (A) The GLX1 and GLX2
624 activity was measured in the total soluble extracts (20 μg protein mL^{-1}) from plant leaves. (B)
625 The transcript abundance was calculated relative to the expression level of the reference gene
626 (*actin2*). Data are presented as means ± SD from three independent experiments. Differences
627 between the plants grown under atmospheric and high [CO_2] were analysed with a Student's
628 *t*-test. Asterisks indicate statistically significant differences at $p < 0.05$.

629

630 **Fig. 4.** Phylogenetic tree of the evolutionary relationship between glyoxalase I (GLX1) in

631 oxygenic phototrophs. Branch lengths correspond to the evolutionary distances. Organisms
632 included in this phylogenetic analysis are S6803, cyanobacterium *Synechocystis* sp. PCC
633 6803; Cv, green alga *Chlorella variabilis*; Mp, liverwort *Marchantia polymorpha*; Sm, fern
634 *Selaginella moellendorffii*; At, C_3 plant *Arabidopsis thaliana*; Os, C_3 plant *Oryza sativa*; Zm,
635 C_4 plant *Zea mays*; Cm, red alga *Cyanidioschyzon merolae*; Pt, diatom *Phaeodactylum*
636 *tricornutum*; Ec, heterotrophic prokaryote *Escherichia coli*; and Sc, heterotrophic eukaryote
637 *Saccharomyces cerevisiae*.
638
639 **Fig. 5.** Phylogenetic tree of the evolutionary relationship among glyoxalase II (GLX2)
640 expressed in oxygenic phototrophs. Branch lengths correspond to the evolutionary distances.
641 Organisms included in this phylogenetic analysis are S6803, cyanobacterium *Synechocystis* sp.
642 PCC 6803; Cv, green alga *Chlorella variabilis*; Mp, liverwort *Marchantia polymorpha*; Sm,
643 fern *Selaginella moellendorffii*; At, C_3 plant *Arabidopsis thaliana*; Os, C_3 plant *Oryza sativa*;
644 Zm, C_4 plant *Zea mays*; Cm, red alga *Cyanidioschyzon merolae*; Pt, diatom *Phaeodactylum*
645 *tricornutum*; Ec, heterotrophic prokaryote *Escherichia coli*; and Sc, heterotrophic eukaryote
646 *Saccharomyces cerevisiae*.
647
648 **Fig. 6.** Proposed metabolic model of the glyoxalase (GLX) system in plant leaves.
649 Abbreviations used: MG, methylglyoxal; TPs, triose phosphates: i.e., glyceraldehyde
650 3-phosphate and dihydroxyacetone; GSH, reduced glutathione; HA, hemithioacetal; and SLG,
651 *S*-D-lactoylglutathione.

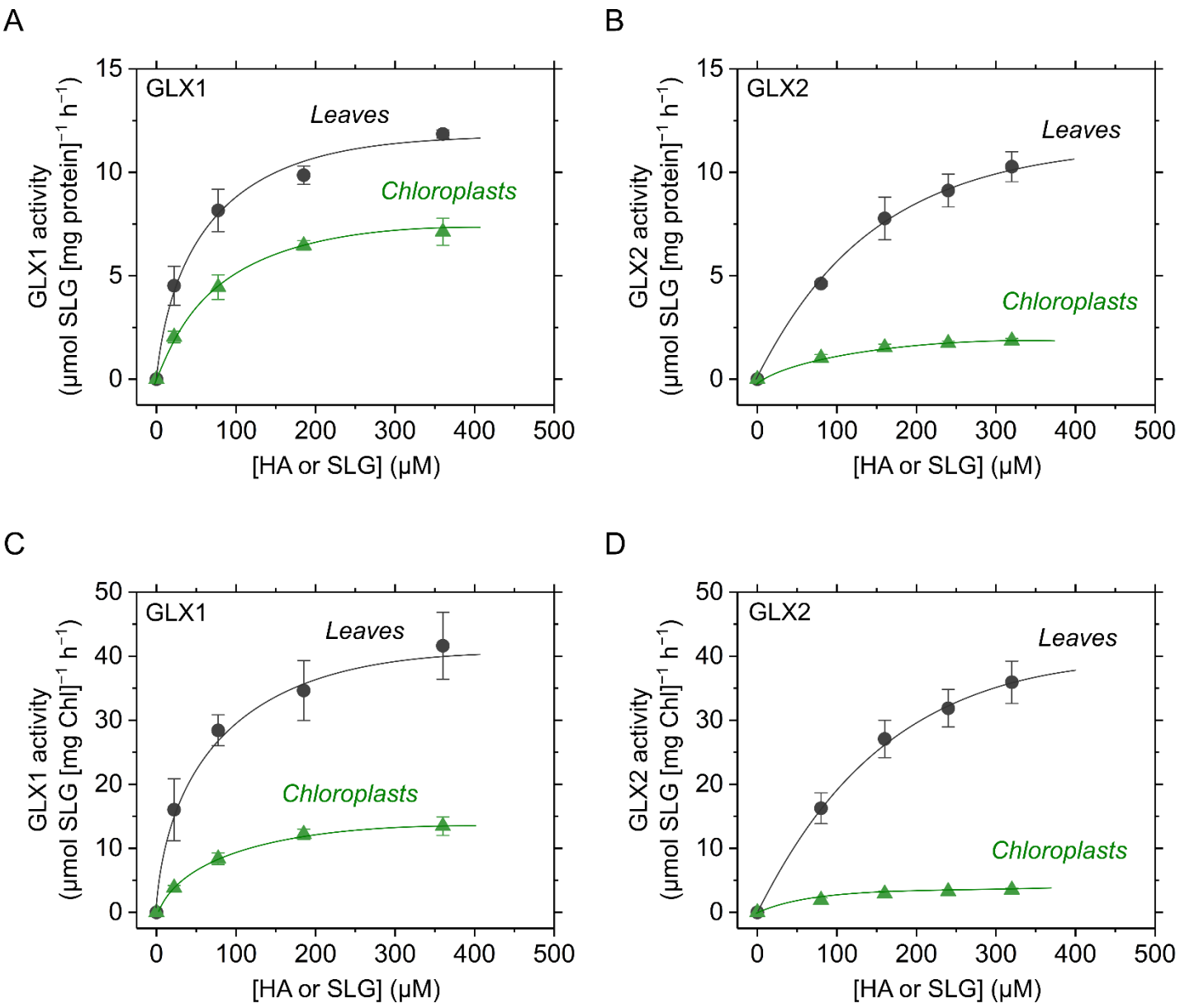

Fig. 1. Dependence of the substrates in the soluble extracts (20 μg protein mL^{-1}) from spinach leaves (grey circles) and chloroplasts (green triangles) on glyoxalase (GLX) 1 (A, C) and 2 (B, D) activities. The activity was estimated based on the amounts of protein (A, B) or chlorophyll (Chl) (C, D). The substrates hemithioacetal (HA) and *S*-D-lactoylglutathione (SLG) were used; the production and consumption rates of SLG were measured for GLX1 and GLX2 activity, respectively. Data are presented as means ± SD from three independent experiments.

Figure 1. Shimakawa et al.

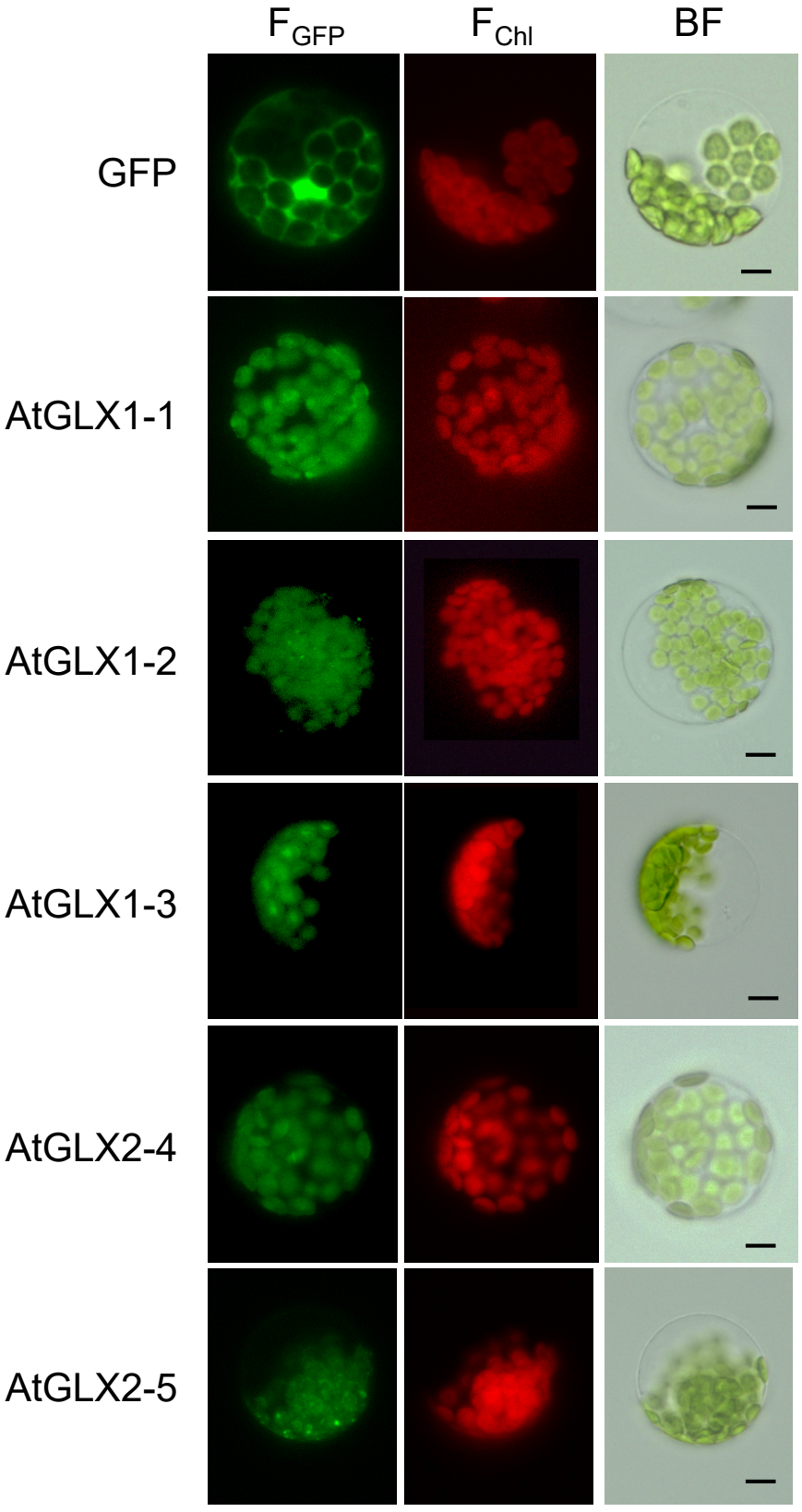

Fig. 2. Subcellular localisation of the GFP-fused glyoxalase (GLX) 1 and 2 proteins expressed in transiently transformed *A. thaliana* mesophyll protoplasts. Fluorescent images of GFP (F_{GFP}), chlorophyll autofluorescence (F_{Chl}), and bright field (BF) are shown. Free GFP protein was used as a control. Black bars = 10 μm.

Figure 2. Shimakawa et al.

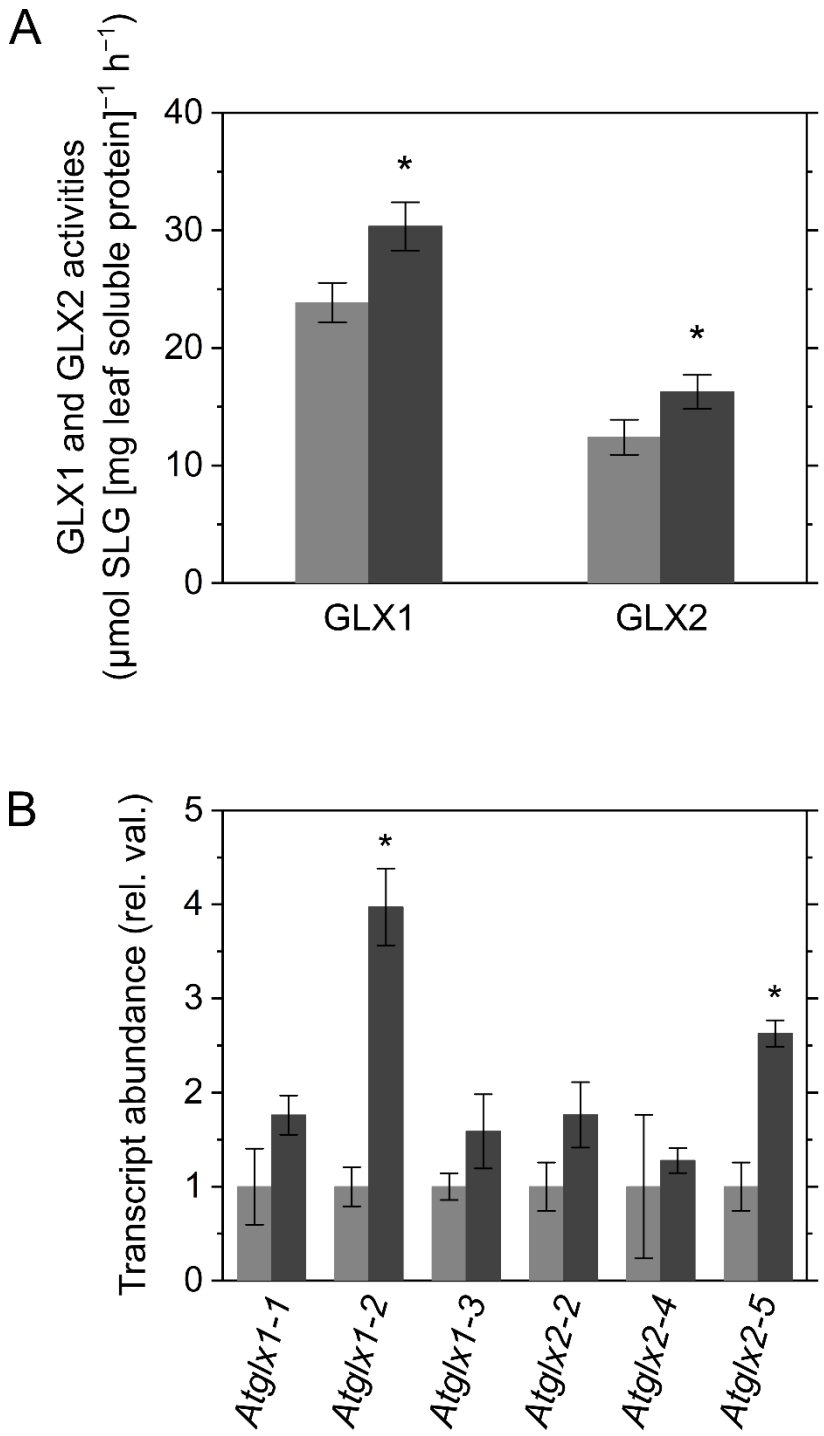

Fig. 3. Activity (A) and expression (B) of glyoxalase (GLX) 1 and 2 in *A. thaliana* leaves in response to the increase in ambient [CO_2]. Wild-type plants were grown at atmospheric (400 ppm, grey bars) and high (2000 ppm, dark grey bars) [CO_2]. (A) The GLX1 and GLX2 activity was measured in the total soluble extracts (20 µg protein mL^{-1}) from plant leaves. (B) The transcript abundance was calculated relative to the expression level of the reference gene (*actin2*). Data are presented as means ± SD from three independent experiments. Differences between the plants grown under atmospheric and high [CO_2] were analysed with a Student's *t*-test. Asterisks indicate statistically significant differences at $p < 0.05$.

Figure 3. Shimakawa et al.

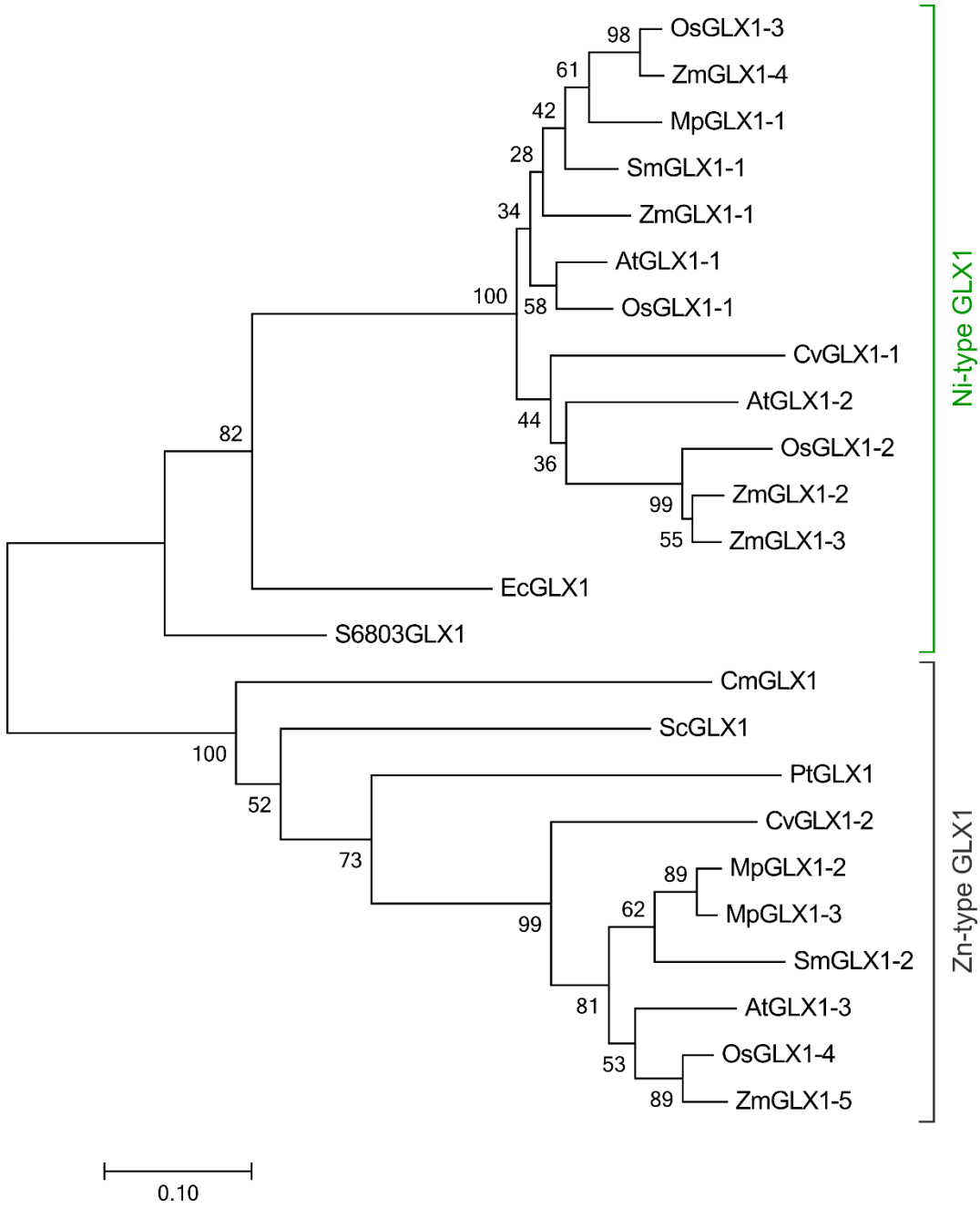

Fig. 4. Phylogenetic tree of the evolutionary relationship between glyoxalase I (GLX1) in oxygenic phototrophs. Branch lengths correspond to the evolutionary distances. Organisms included in this phylogenetic analysis are S6803, cyanobacterium *Synechocystis* sp. PCC 6803; Cv, green alga *Chlorella variabilis*; Mp, liverwort *Marchantia polymorpha*; Sm, fern *Selaginella moellendorffii*; At, C_3 plant *Arabidopsis thaliana*; Os, C_3 plant *Oryza sativa*; Zm, C_4 plant *Zea mays*; Cm, red alga *Cyanidioschyzon merolae*; Pt, diatom *Phaeodactylum tricornutum*; Ec, heterotrophic prokaryote *Escherichia coli*; and Sc, heterotrophic eukaryote *Saccharomyces cerevisiae*.

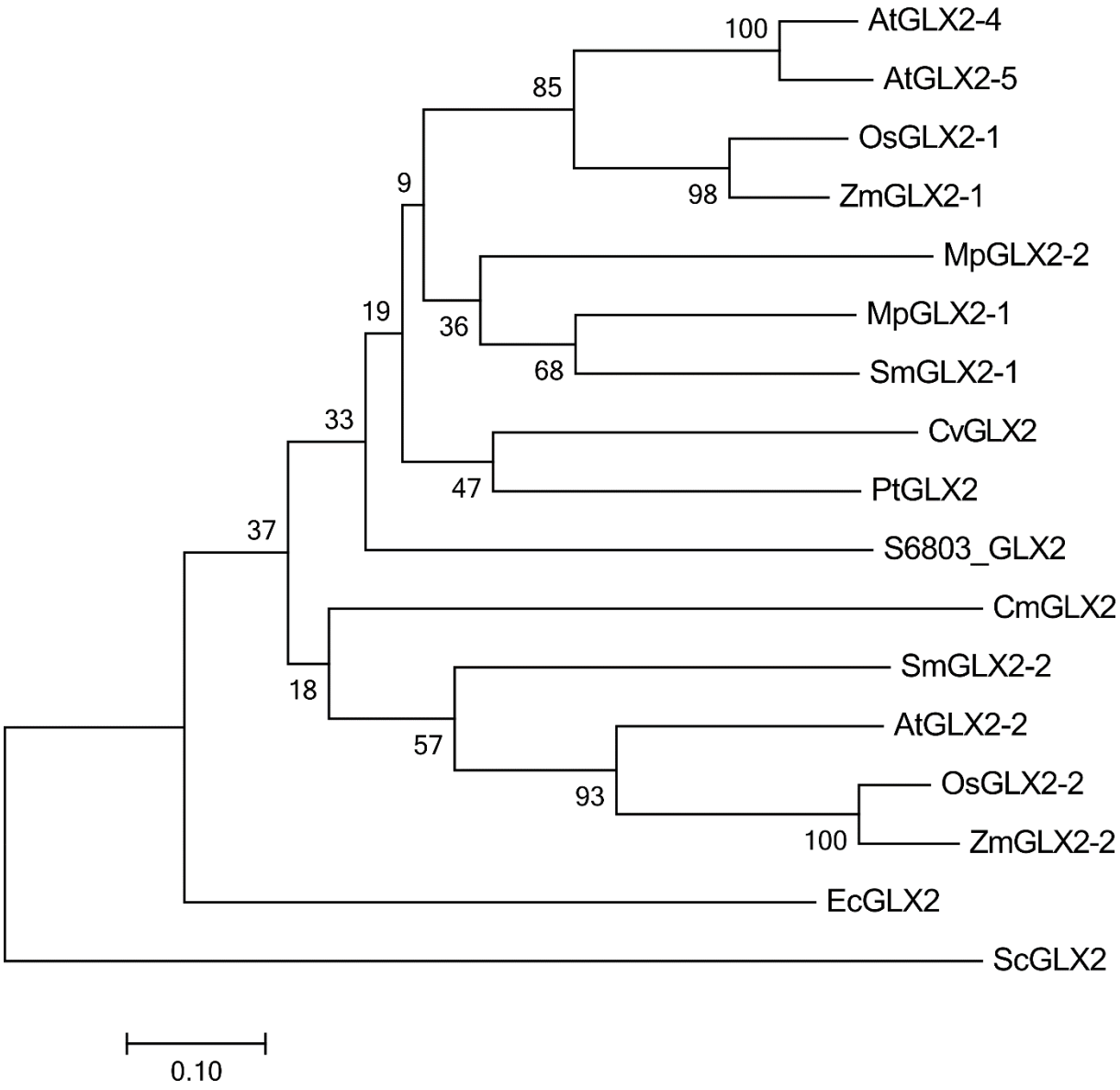

Fig. 5. Phylogenetic tree of the evolutionary relationship between glyoxalase II (GLX2) expressed in oxygenic phototrophs. Branch lengths correspond to the evolutionary distances. Organisms included in this phylogenetic analysis are S6803, cyanobacterium *Synechocystis* sp. PCC 6803; Cv, green alga *Chlorella variabilis*; Mp, liverwort *Marchantia polymorpha*; Sm, fern *Selaginella moellendorffii*; At, C_3 plant *Arabidopsis thaliana*; Os, C_3 plant *Oryza sativa*; Zm, C_4 plant *Zea mays*; Cm, red alga *Cyanidioschyzon merolae*; Pt, diatom *Phaeodactylum tricornutum*; Ec, heterotrophic prokaryote *Escherichia coli*; and Sc, heterotrophic eukaryote *Saccharomyces cerevisiae*.

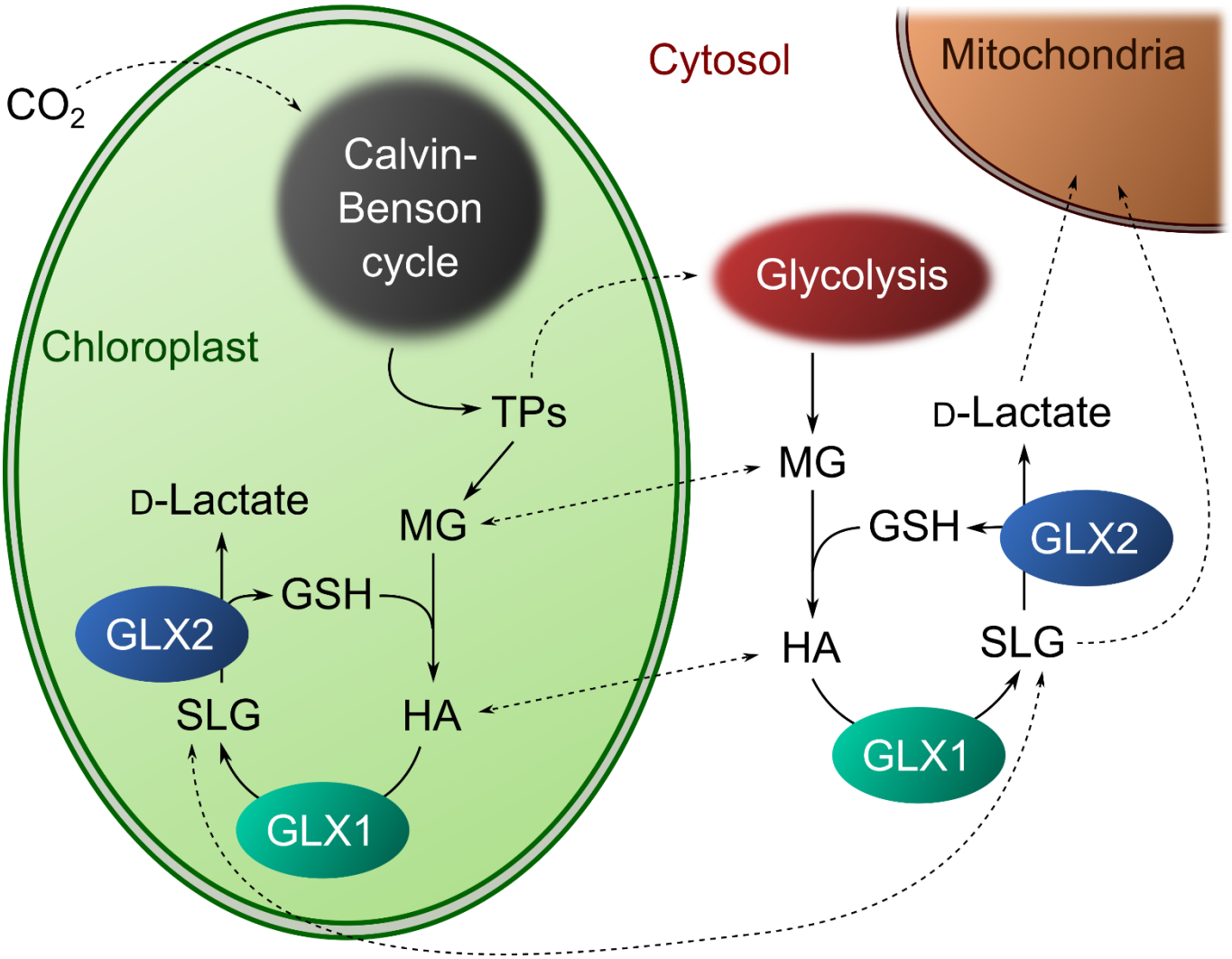

Fig. 6. Proposed metabolic model of the glyoxalase (GLX) system in plant leaves. Abbreviations used: MG, methylglyoxal; TPs, triose phosphates: i.e., glyceraldehyde 3-phosphate and dihydroxyacetone; GSH, reduced glutathione; HA, hemithioacetal; and SLG, *S*-D-lactoylglutathione.

Figure 6. Shimakawa et al.

Supplemental Table S1. Primers used in this study

Name	Sequences (5'−3')
P1: GstGLX2-4 f	GGTTCCGCGTGGATCCATGCAAATTGAACTGGTGCCATGTC
P2: GstGLX2-4 r	GGGAATTCGGGGATCCTAAGCTTTGAAATTGTCCTTTG
P3: sGLX1-1Gfp f	TACAATTACAGTCGACATGAGTTCGTACTCAATAGCAAGT
P4: GLX1-1Gfp f	TACAATTACAGTCGACATGGCGTCGGAAGCGAGG
P5: GLX1-1Gfp r	CCCTTGCTCACCATGGCAGCTGCGTTTACGGTAGTA
P6: sGLX1-2Gfp f	TACAATTACAGTCGACATGAATGAGATTGCTTCCGCCTC
P7: GLX1-2Gfp f	TACAATTACAGTCGACATGGCTGAGGCTTCTGATTTGTT
P8: GLX1-2Gfp r	CCCTTGCTCACCATGGCTTCCAGTTCCTTGAGAAAATCTT
P9: sGLX1-3Gfp f	TACAATTACAGTCGACATGCTTCATGTTGTTTATCGTGT
P10: GLX1-3Gfp f	TACAATTACAGTCGACATGGTGAGGATCATTCCTATGGC
P11: GLX1-3Gfp r	CCCTTGCTCACCATGGCCTCCAGTTCTTGAGAAAGTCAA
P12: GLX2-4Gfp f	TACAATTACAGTCGACATGCAAGCCATCTCCAAAGTT
P13: GLX2-4Gfp r	CCCTTGCTCACCATGGCAGCTTTGAAATTGTCCTTTGCTCT
P14: GLX2-5Gfp f	TACAATTACAGTCGACATGCAAACCATCTCGAAAGCTTC
P15: GLX2-5Gfp r	CCCTTGCTCACCATGGCGAAATCATCCTTTGCTTTCCG
P16: qActin2 f	TCAGATGCCCAGAAGTCTTGTTCC
P17: qActin2 r	CCGTACAGATCCTTCCTGATATCC
P18: qGLX1-1 f	ATGGCGTCGGAAGCGAGGGA
P19: qGLX1-1 r	CCAGCACACGTGAGTAAAAGTCA
P20: qGLX1-2 f	TGTCGTGCTATGTGTGTGTGC
P21: qGLX1-2 r	AAACCGTCCATAACCGCAAA
P22: qGLX1-3 f	GAGGAGAGGCCTTGTTGTGAA
P23: qGLX1-3 r	GACGCAACATAGGCTTTTATACTG
P24: qGLX2-4 f	GCGATCCTGGTTTAATCTGTAA
P25: qGLX2-4 r	CGAGGGTTCATCAAAGTAGAAAC
P26: qGLX2-5 f	CATTCCAGAGGCCGCAGATG
P27: qGLX2-5 r	GGTGCACACTCATTTGAGGAC

Supplemental Table S2. Kinetic parameter of the recombinant S6803GLX1

	K_m (mM)	k_{cat} (min^{-1})	k_{cat}/K_m (mM^{-1} min^{-1})
S6803GLX1			
*In the absence of Ni^{2+}	0.39 ± 0.10	350 ± 30	910
In the presence of Ni^{2+}	0.018 ± 0.001	10500 ± 1500	590000

For the measurement of the recombinant S6803GLX1 protein (0.05 μg mL^{-1}), hemithioacetal was used as the substrate. Data are means ± SD for three independent experiments. *Shimakawa et al. (2013).

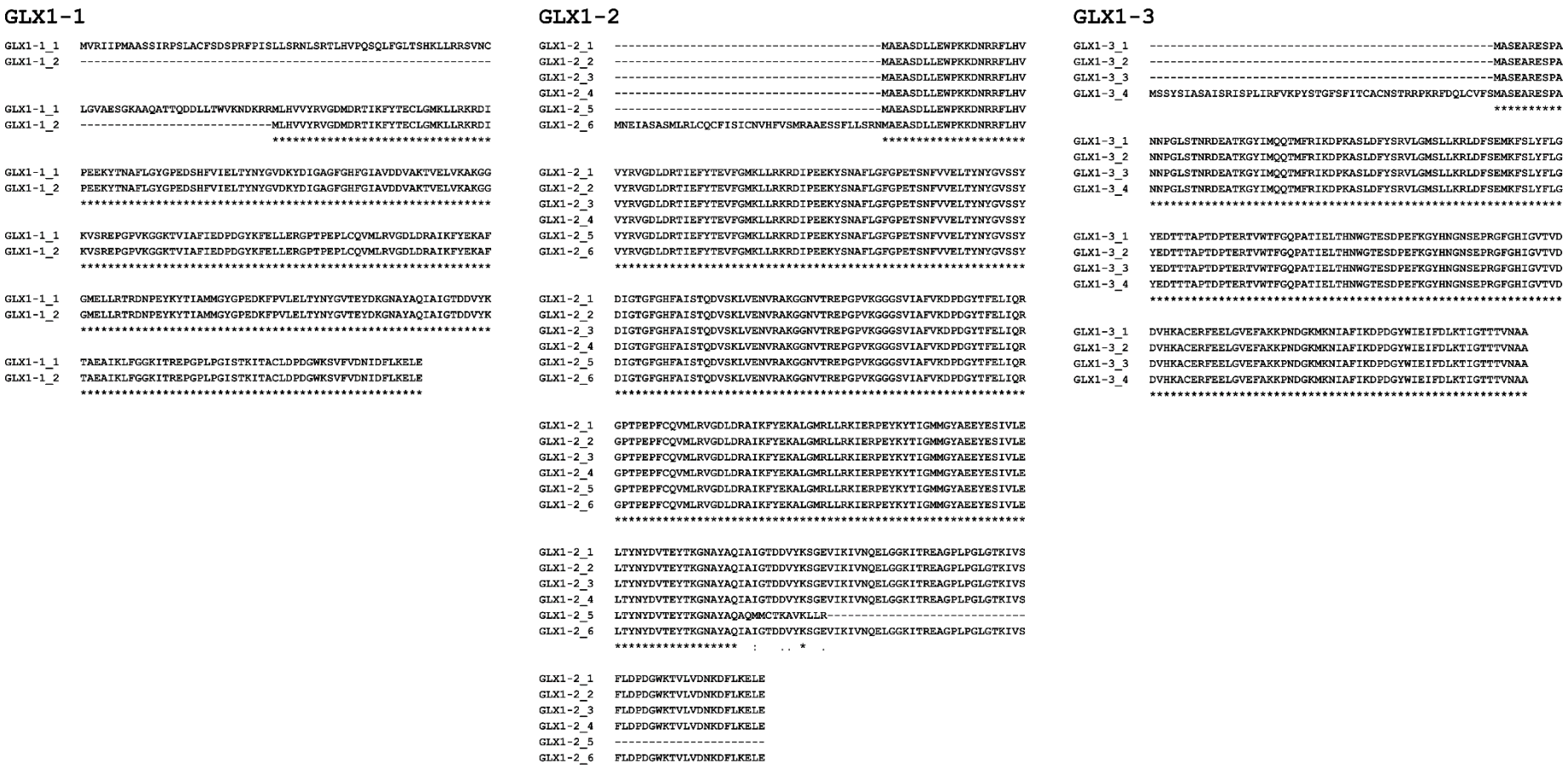

Supplemental Fig. S1. Amino acid sequences for each AtGLX1 splice variant.

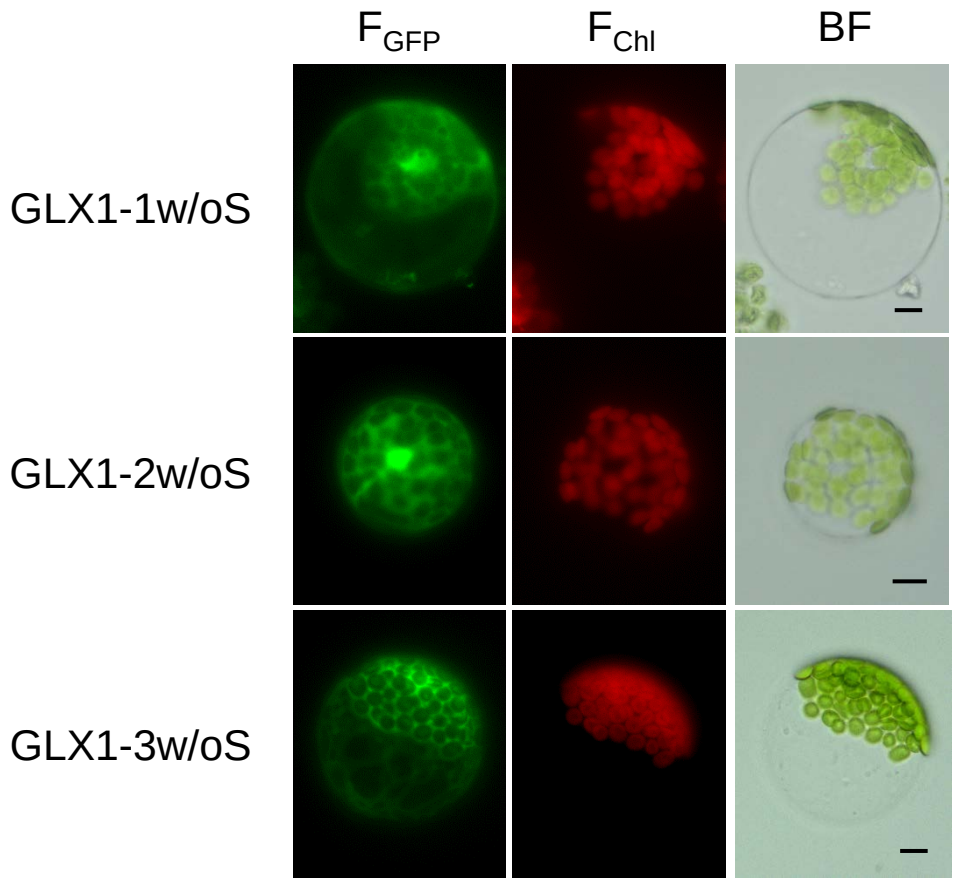

Supplemental Fig. S2. Subcellular localisation of GLX1w/oS–GFP fusion proteins expressed in *A. thaliana* mesophyll protoplasts. Fluorescence images of GFP (F_{GFP}), chlorophyll autofluorescence (F_{Chl}), and the bright field (BF) are shown. Black bars = 10 µm.

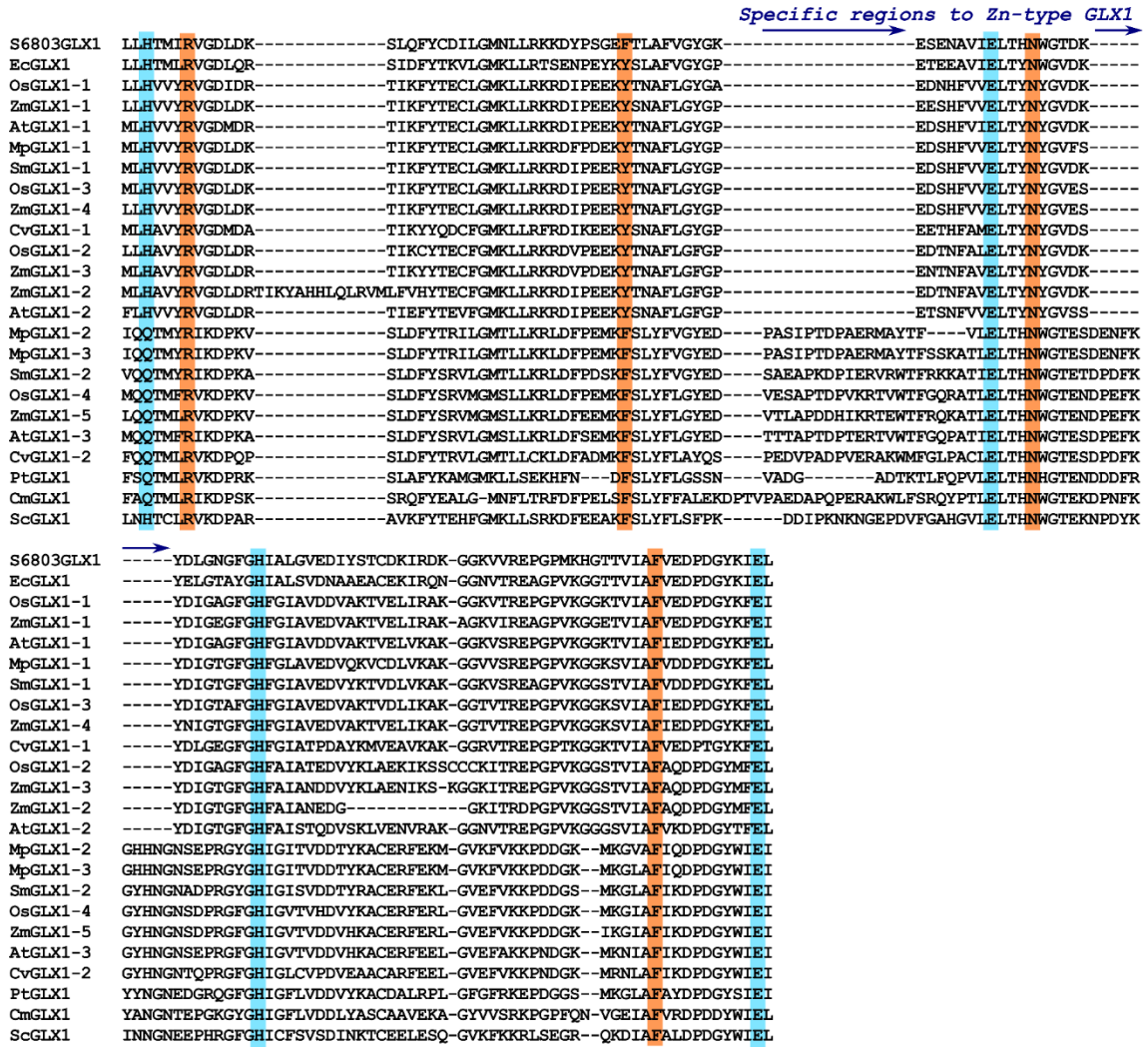

Supplemental Fig. S3. Sequence comparison of the Glyoxalase domain (Pfam, PF00903) in the N-terminus of glyoxalase I (GLX1) among oxygenic phototrophs. Blue shading represents the metal-binding sites; orange shading represents substrate-binding sites. Navy arrows indicate the regions specific to Zn^{2+}-dependent GLX1. S6803, cyanobacterium *Synechocystis* sp. PCC 6803; Cv, green alga *Chlorella variabilis*; Mp, liverwort *Marchantia polymorpha*; Sm, fern *Selaginella moellendorffii*; At, C_3 plant *Arabidopsis thaliana*; Os, C_3 plant *Oryza sativa*; Zm, C_4 plant *Zea mays*; Cm, red alga *Cyanidioschyzon merolae*; Pt, diatom *Phaeodactylum tricornutum*; Ec, heterotrophic prokaryote *Escherichia coli*; and Sc, heterotrophic eukaryote *Saccharomyces cerevisiae*.

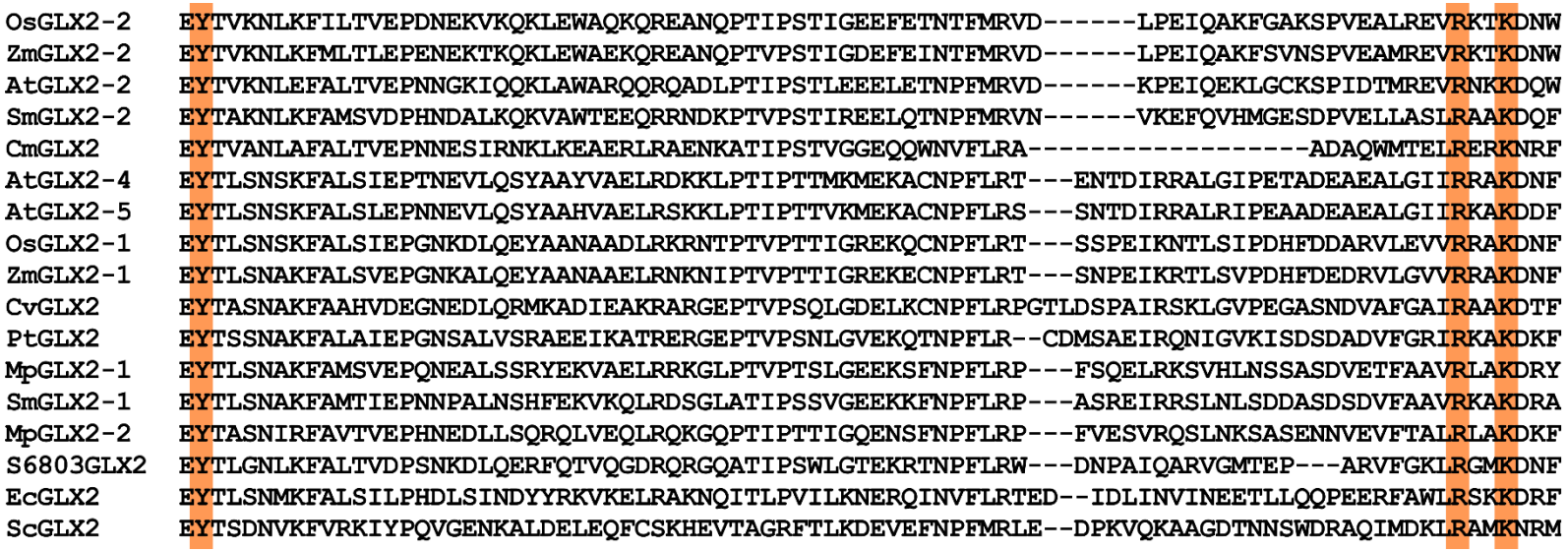

Supplemental Fig. S4. Sequence comparison of the hydroxyacylglutathione hydrolase domain (Pfam, PF16123) in the C-terminus of glyoxalase II (GLX2) among oxygenic phototrophs. Orange shading indicates substrate-binding sites. S6803, cyanobacterium *Synechocystis* sp. PCC 6803; Cv, green alga *Chlorella variabilis*; Mp, liverwort *Marchantia polymorpha*; Sm, fern *Selaginella moellendorffii*; At, C_3 plant *Arabidopsis thaliana*; Os, C_3 plant *Oryza sativa*; Zm, C_4 plant *Zea mays*; Cm, red alga *Cyanidioschyzon merolae*; Pt, diatom *Phaeodactylum tricornutum*; Ec, heterotrophic prokaryote *Escherichia coli*; and Sc, heterotrophic eukaryote *Saccharomyces cerevisiae*.